

# Rapidity evolution of the entanglement entropy in quarkonium: parton and string duality

Yizhuang Liu\*

*Institute of Theoretical Physics, Jagiellonian University, 30-348 Kraków, Poland*

Maciej A. Nowak†

*Institute of Theoretical Physics and Mark Kac Center for Complex Systems Research,  
Jagiellonian University, 30-348 Kraków, Poland*

Ismail Zahed‡

*Center for Nuclear Theory, Department of Physics and Astronomy,  
Stony Brook University, Stony Brook, New York 11794-3800, USA*

We investigate the quantum entanglement in rapidity space of the soft gluon wave function of a quarkonium, in theories with non-trivial rapidity evolutions. We found that the rapidity evolution drastically changes the behavior of the entanglement entropy, at any given order in perturbation theory. At large  $N_c$ , the reduced density matrices that “resum” the leading rapidity-logs can be explicitly constructed, and shown to satisfy Balitsky-Kovchegov (BK)-like evolution equations. We study their entanglement entropy in a simplified 1+1 toy model, and in 3D QCD. The entanglement entropy in these cases, after re-summation, is shown to saturate the Kolmogorov-Sinai bound of 1. Remarkably, in 3D QCD the essential growth rate of the entanglement entropy is found to vanish at large rapidities, a result of kinematical “quenching” in transverse space. The one-body reduction of the entangled density matrix obeys a BFKL evolution equation, which can be recast as an evolution in an emergent AdS space, at large impact-parameter and large rapidity. This observation allows the extension of the perturbative wee parton evolution at low- $x$ , to a dual non-perturbative evolution of string bits in curved AdS<sub>5</sub> space, with manifest entanglement entropy in the confining regime.

## I. INTRODUCTION

Quantum entanglement permeates most of our quantum description of physical laws. It follows from the fact that quantum states are mostly superposition states, and two non-causally related measurements can be correlated, as captured by the famed EPR paradox. A quantitative measure of this correlation is given by the quantum entanglement entropy. The entanglement entropy of quantum many body system and quantum field theory has been extensively explored in the literature [1–5].

In hadron physics, quantum entanglement is inherent to any hadron state, which is made more spectacular on the light-front with luminal wave-functions. Unlike a generic

---

\* [yizhuang.liu@uj.edu.pl](mailto:yizhuang.liu@uj.edu.pl)

† [maciej.a.nowak@uj.edu.pl](mailto:maciej.a.nowak@uj.edu.pl)

‡ [ismail.zahed@stonybrook.edu](mailto:ismail.zahed@stonybrook.edu)

quantum many body system, quantum field theory is intrinsically multi-scale in nature which leads to non-trivial evolutions with respect to energy and rapidity scales. In particular, in 4D gauge theories, under large boosts, the wave-functions pile more and more *small- $x$  partons* or *wee partons* [6] and results in nontrivial asymptotic behaviors in physical cross sections.

A comprehensive understanding of the small- $x$  asymptotics in 4D gauge theory, is still not available in so far even in perturbation theory, but there are progresses. In weak coupling QCD, the rapidity evolution is extensively discussed in the literature, leading to various evolutions equations such as the BFKL equation [7–9] or the BK equations [10, 11]. In strong coupling QCD, they are identified with *string bits* [12–14], and well described by a stringy evolution equation in the double limit of strong gauge coupling and large  $N_c$ . The general idea is, the small- $x$  partons behave very differently with respect to the large- $x$  spectators and likely to be described by an emergent effective theory. A natural question is then, since they are both quantum degrees of freedom in the original QFT, how the small- $x$  and large- $x$  partons entangle with each other and how the entanglement is related to experiments.

The entanglement entropy in diffractive  $ep$  or  $pp$  scattering was first noted in the strong coupling regime using a holographic string analysis [15] (called quantum entropy there), and in weak coupling using the evolution equation based analysis [16]. In both cases, the entanglement entropy was found to be extensive in the rapidity, an observation made since by many others in perturbative QCD [17, 18]. The large entanglement entropy stored in hadrons and nuclei, may explain the prompt entropies released in current hadron colliders, in the form of large particle multiplicities [19–22]. For completeness, we note that an entropy composed of the multiplicities of the produced gluons in the context of saturation models was also discussed in [23].

Recently, we have used 2D QCD in the large  $N_c$  limit, to analyze quantum entanglement in confined meson states [22]. The entanglement entropy in parton- $x$  was found to be also extensive in the meson rapidity, but with a central-charge-like played by the cumulative quark PDF, and hence dependent on the fraction of parton- $x$  measured. Much like in 4D, the entanglement entropy exhibits an asymptotic expansion that is similar to the one observed for meson-meson scattering in the Regge limit. Most notably, the entanglement entropy per unit rapidity in a 2D nucleus (a sum of longitudinal mesons on the light front) was found to be at the bound set for quantum information flow [24, 25].

The purpose of this work is to extend some of our recent 2D QCD observations [22], to 4D QCD where non-trivial rapidity divergences are the lore at weak coupling, and closely related to the Regge behavior of scattering amplitudes. We will mostly focus on the entanglement entropy in a quarkonium state at next to leading order in the weak coupling  $\alpha_s$ , and show that the rapidity divergences are at the origin of double logarithms in rapidity. This observation is readily extended to higher orders, and re-summed through an evolution equation in the large  $N_c$  limit. An analysis of the proton wave function with

a similar motivation was recently discussed in [26].

The outline of the paper is as follows: in section II we outline the construction of the reduced density matrix for a quarkonium state in leading order in  $\alpha_s$ . In section III, we derive the reduced density matrix for the soft gluon, by tracing over the quark sources. The ensuing entanglement entropy receives contributions from both the real and virtual parts of the wavefunction, but the latter generates double logarithms in rapidity as naturally expected. In section IV, we show how to resum the leading rapidity logarithms in the entanglement entropy. In the large  $N_c$  limit and weak coupling, the density matrices with and without overall longitudinal momentum conservation, are shown to obey BK-like evolution equations. The ensuing entanglement entropy is found to saturate the Kolmogorov-Sinai bound of 1, for the case after partial tracing which imposing momentum conservation, but otherwise linear in the rapidity. The evolution equation can be solved explicitly for non-conformal QCD in 3D. The rate of growth of the entanglement entropy is shown to vanish at large rapidities, a consequence of the shrinking of the transverse phase space. In section V, we show that the evolution of the trace of the density matrix obeys a standard BFKL evolution equation, which can be mapped on an evolution in an emergent AdS<sub>3</sub> space. In section VI, we extend this observation to the strong coupling regime, where the evolution is captured by the tachyonic mode of a quantum string in AdS<sub>5</sub>, where the string bits are dual to the wee partons. Our conclusions are in section VII.

## II. QUARKONIUM WAVE FUNCTION

In this section we study the rapidity-space entanglement of the light front wave function (LFWF) for a pair of a heavy quark and anti-quark. The same system has been investigated in the literature, to derive the non-linear rapidity evolution equation of the dipole generating functional [27, 28]. It has also been revisited recently, to provide a concrete example for the formulation of LFWF amplitudes [29].

Unlike the 2D case where there is no rapidity divergences in the light front (LF) quantization, in 4D gauge theory there are non-trivial rapidity divergences (RD). They are closely related to the Regge limit of gauge theory. Still, they are not totally understood from first principles, even in perturbation theory (PT).

On the LF, the soft gluon wave function of a  $\bar{Q}Q$  pair, to leading order is of the form [27, 30]

$$|\bar{Q}Q\rangle = |\bar{Q}Q\rangle^0 + |\bar{Q}Q\rangle^{(1)} + |\bar{Q}Qg\rangle, \quad (1)$$

Here

$$|\bar{Q}Q\rangle^{(0)} = \frac{1}{\sqrt{\Lambda^-}\sqrt{V_\perp}} \sum_{z, \vec{k}_\perp} \frac{1}{\sqrt{(2\pi)^2}} \Psi_{\sigma, \sigma'}^{(0)}(z, \vec{k}_\perp) |z, \sigma, \vec{k}_\perp\rangle_Q \otimes |\bar{z}, \sigma', -\vec{k}_\perp\rangle_{\bar{Q}}, \quad (2)$$

is the leading order quarkonium wave function with initial profile  $\Psi_{\sigma,\sigma'}^{(0)}(z, \vec{k}_\perp)$ . The free-Fock basis is normalized as  $\langle z|z'\rangle = \delta_{z,z'}$ , and the momentum fraction relates to the discrete LF label  $n$  through the relation

$$z = \frac{2n+1}{2\Lambda^-} . \quad (3)$$

Comparing with the standard notation in the literature, we have absorbed a factor of  $1/\sqrt{z(1-z)}$  into the definition of the LFWF, which will generate precisely the Lorentz invariant LF phase space measure

$$\int_{z_{\min}}^1 \frac{dz}{z} , \quad (4)$$

after squaring. Again, the natural rapidity cutoff  $z_{\min}$  is given by the inverse of  $\Lambda^-$ . We assume that the leading WF  $\Psi^{(0)}$  is supported well away from  $z=0$ , for instance it can be a pair of free quarks with fixed momentum fractions  $z=z_0 \sim \frac{1}{2}$ , and zero transverse momenta  $\vec{k}_\perp=0$ . More specifically,  $\Psi^{(0)} = \delta_{z,z_0} \delta_{\vec{k}_\perp,0}$ , which is the case considered before when formulating the LFWF amplitudes.

The most interesting contribution in (1) is the soft-gluon contribution. Using the standard rule in LFPT, one can show that the leading soft gluon contribution to the LFWF is

$$|\bar{Q}Qg\rangle = \frac{1}{\Lambda^- V_\perp} \sum_{z,x,k_\perp,k_g,\epsilon,\alpha} \Psi^\alpha(x,z,\vec{k}_\perp,\vec{k}_{g,\perp},\vec{\epsilon}) |z,\vec{k}_\perp,\sigma\rangle_Q |\bar{z}-x,-\vec{k}_\perp-\vec{k}_{g,\perp},\sigma'\rangle_{\bar{Q}} |x,\vec{k}_{g,\perp},\vec{\epsilon},\alpha\rangle_g , \quad (5)$$

where one has

$$\Psi^\alpha(x,z,\vec{k}_\perp,\vec{k}_{g,\perp},\vec{\epsilon}) = \frac{2gt^a \vec{\epsilon}^* \cdot \vec{k}_{g,\perp}}{\sqrt{x} k_{g,\perp}^2} \left( \Psi_{\sigma,\sigma'}^{(0)}(z,\vec{k}_\perp + \vec{k}_{g,\perp}) - \Psi_{\sigma,\sigma'}^{(0)}(z,\vec{k}_\perp) \right) . \quad (6)$$

Notice that the above equation applies to any transverse dimensions, in particular, for  $D_\perp=2$  the wave function can be written in coordinate space as

$$\begin{aligned} \Psi^\alpha(x,z,\vec{b}_{1\perp},\vec{b}_{2\perp}) &= \int \frac{d^2k_\perp d^2k_{g,\perp}}{(2\pi)^4} e^{i\vec{k}_\perp \cdot \vec{b}_{10\perp} + i\vec{k}_{g,\perp} \cdot \vec{b}_{20\perp}} \Psi^\alpha(x,z,\vec{k}_\perp,\vec{k}_{g,\perp},\vec{\epsilon}) \\ &= \frac{igt^a}{\pi\sqrt{x}} \Psi^0(z,\vec{b}_{1\perp})_{\sigma,\sigma'} \vec{\epsilon}^* \cdot \left( \frac{\vec{b}_{21}}{|\vec{b}_{21}|^2} - \frac{\vec{b}_{20}}{|\vec{b}_{20}|^2} \right) , \end{aligned} \quad (7)$$

with  $\vec{b}_{21} = \vec{b}_{2\perp} - \vec{b}_{1\perp}$ ,  $\vec{b}_{10} = \vec{b}_{1\perp} - \vec{b}_{0\perp}$  and  $\vec{b}_{20} = \vec{b}_{2\perp} - \vec{b}_{0\perp}$ . This is the real part of the wave function. The norm of this state is given by

$$\langle \bar{Q}Qg | \bar{Q}Qg \rangle = \frac{2\alpha_s C_F}{\pi} \int d^2b_\perp \ln b_\perp^2 \mu^2 \times \int_{x_{\min}}^{x_0} \frac{dx}{x} \times \int dz \sum_{\sigma,\sigma'} |\Psi^0(z,\vec{b}_{1\perp})_{\sigma,\sigma'}|^2 . \quad (8)$$

There is a UV divergence which is regularized by the cutoff  $\mu$ , and the rapidity divergence is cutoff by  $x_{\min} = \frac{1}{2\Lambda^-}$ . On the other hand, the virtual part  $|\bar{Q}Q\rangle^{(1)}$  can be written with the following wave function

$$\Psi^{(1)}(z, \vec{b}_\perp, \sigma, \sigma') = -\frac{\alpha_s C_F}{\pi} \ln b_\perp^2 \mu^2 \times \int_{x_{\min}}^{x_0} \frac{dx}{x} \times \Psi^0(z, \vec{b}_\perp, \sigma, \sigma'), \quad (9)$$

With this in mind, it is clear that when squaring (1), the real and virtual parts cancel, in agreement with perturbative unitarity.

### III. SOFT-GLUON ENTANGLEMENT ENTROPY IN QUARKONIUM

In our previous work in 2D QCD [22], we found that for a meson state quantized in the discrete LF quantization, the entanglement entropy in rapidity space is finite in the ultra-violet, but contains a logarithmic divergent term in the effective box size  $\Lambda^- = P^+ L^-$ , which is identified with the meson rapidity. In this section, we investigate the rapidity space entanglement for the quarkonium or  $\bar{Q}Q$  system in 4D perturbative QCD. We show that the non-trivial rapidity divergence (or rapidity transcendentality) leads to an enhanced divergence in  $\ln \Lambda^-$ . At order  $\alpha_s$  the leading contribution is enhanced by  $\ln^2 \Lambda^-$ , and at order  $\alpha_s^k$  it is enhanced by  $(\ln \Lambda^-)^{1+k}$ . We first consider the order  $\alpha_s$  case, and then generalize to order  $\alpha_s^k$ .

#### A. Leading order in $\alpha_s$

With the one-loop soft gluon part of the wave function at hand, we can now perform partial tracing, to obtain the reduced density matrix. We trace over the quark longitudinal and transverse contributions, leaving the gluon longitudinal contribution in the final state untraced,

$$\begin{aligned} \hat{\rho} = & |0\rangle\langle 0| \left( 1 - \frac{2\alpha_s C_F}{\pi} \int d^2 b_\perp \ln b_\perp^2 \mu^2 \times \int_{x_{\min}}^{x_0} \frac{dx}{x} \times \int dz \sum_{\sigma, \sigma'} |\Psi^0(z, \vec{b}_\perp)_{\sigma, \sigma'}|^2 \right) \\ & + \frac{1}{\Lambda^-} \sum_{x < x_0} \frac{1}{x} |x\rangle_g \langle x|_g \times \left( \frac{2\alpha_s C_F}{\pi} \times \int d^2 b_\perp \ln b_\perp^2 \mu^2 \times \int dz \sum_{\sigma, \sigma'} |\Psi^0(z, \vec{b}_\perp)_{\sigma, \sigma'}|^2 \right) \end{aligned} \quad (10)$$

Clearly, the off-diagonal term in the gluon longitudinal momentum, vanishes in the trace to this order.

With the reduced density matrix, we now compute the entanglement entropy. The

virtual or vacuum part leads to the result

$$\begin{aligned}
S_{\text{virtual}} &= - \left( 1 - \frac{2\alpha_s C_F}{\pi} \int d^2 b_{\perp} \ln b_{\perp}^2 \mu^2 \times \int_{x_{\min}}^{x_0} \frac{dx}{x} \times \int dz \sum_{\sigma, \sigma'} |\Psi^0(z, \vec{b}_{\perp})_{\sigma, \sigma'}|^2 \right) \\
&\quad \times \ln \left( 1 - \frac{2\alpha_s C_F}{\pi} \int d^2 b_{\perp} \ln b_{\perp}^2 \mu^2 \times \int_{x_{\min}}^{x_0} \frac{dx}{x} \times \int dz \sum_{\sigma, \sigma'} |\Psi^0(z, \vec{b}_{\perp})_{\sigma, \sigma'}|^2 \right) \\
&= \frac{2\alpha_s C_F}{\pi} \int d^2 b_{\perp} \ln b_{\perp}^2 \mu^2 |\Psi^{(0)}(b_{\perp})|^2 \times \int_{x_{\min}}^{x_0} \frac{dx}{x} + \mathcal{O}(\alpha_s^2) .
\end{aligned} \tag{11}$$

where  $|\Psi^{(0)}(b_{\perp})|^2 \equiv \int dz \sum_{\sigma, \sigma'} |\Psi^{(0)}(z, b_{\perp})_{\sigma, \sigma'}|^2$  is the initial dipole wave function integrated over  $z$ , and the rapidity divergence (RD) contribution reads

$$\int_{x_{\min}}^{x_0} \frac{dx}{x} \rightarrow \sum_{n=n_0}^{\Lambda^{-1/2}} \frac{1}{n + \frac{1}{2}} = \ln \Lambda^{-} x_0 + C . \tag{12}$$

On the other hand, what is more interesting is the contribution from the real emission. In terms of

$$p_0 = \frac{2\alpha_s C_F}{\pi} \int d^2 b_{\perp} \ln b_{\perp}^2 \mu^2 |\Psi^{(0)}(b_{\perp})|^2 , \tag{13}$$

the real contribution to the entanglement entropy is

$$S_{\text{real}} = \ln \Lambda^{-} \times p_0 \times \int_{x_{\min}}^{x_0} \frac{dx}{x} - \int_{x_{\min}}^{x_0} \frac{dx}{x} p_0 \ln \frac{p_0}{x} \rightarrow \frac{1}{2} \ln^2 \Lambda^{-} p_0 + \ln \Lambda^{-} p_0 \ln \frac{x_0}{p_0} + C \tag{14}$$

The entanglement entropy is now dominated by the double-logarithmic divergent term

$$S_{\text{real}} + S_{\text{virtual}} = \frac{1}{2} \ln^2 \Lambda^{-} p_0 + \ln \Lambda^{-} p_0 \ln \frac{x_0}{p_0} + p_0 \ln \Lambda^{-} x_0 + C . \tag{15}$$

It is the RD that leads to the enhancement of the logarithmic dependency on  $\Lambda^{-}$ . It is also divergent in UV.

## B. Higher order in $\alpha_s$

We now generalize the result to all orders, to extract the leading  $\alpha_s \ln \Lambda^{-}$  contribution. The above suggests the  $\alpha_s^k \ln(\Lambda^{-})^{k+1}$  as the general pattern, which can be shown as follows. First, to obtain the leading  $\ln \Lambda^{-}$  contribution, it is much better if all the gluons are non-traced, namely, more soft gluons in the final state, more logarithms in  $\Lambda$ . Therefore we do not perform partial tracing in gluons. However, the quarks should be traced out, which leads to the structure of the entanglement density matrix in the following form

$$\rho = \sum_n p_n \rho_n , \tag{16}$$

where  $p_n$  is the total probability of finding  $n$ -soft gluons, and the  $\rho_n$  is an effective reduced density matrix with  $n$ -soft gluon on the left and right. Notice that the off-diagonal terms in particle numbers simply vanish, thanks to the total trace in the transverse momentum or color. From (16) the entanglement entropy for  $\rho$  can be found to be

$$S = - \sum_n p_n \ln p_n + \sum_n p_n S_n , \quad (17)$$

where  $S_n = -\text{tr} \rho_n \ln \rho_n$  is the entanglement entropy of the reduced density matrix in the  $n$ -particle sector. For purely real soft emissions, the probability of the state is proportional to

$$p_n \sim \alpha_s^n \int_{x_{\min}}^{x_0} \frac{dx_1}{x_1} \int_{x_1}^{x_0} \frac{dx_2}{x_2} \dots \int_{x_{n-1}}^{x_0} \frac{dx_n}{x_n} \propto \alpha_s^n \ln^n \Lambda^- , \quad (18)$$

and adding virtual corrections will correct it in powers of  $\alpha_s \ln \Lambda^-$  to leading log accuracy. On the other hand, for the purely real soft emissions one can show that

$$\rho_{n,real} \propto \sum_{x_1 \gg x_2 \dots \gg x_n; x_1 \gg x'_2 \dots \gg x'_n} \frac{1}{x_1 \sqrt{x_2 x'_2 \dots x_n x'_n}} |x_1\rangle \dots |x_n\rangle \langle x_1| \dots \langle x'_n| , \quad (19)$$

which involves  $\Lambda^-$  pure states and consequently  $S_n \propto \ln \Lambda^-$ . When multiplied by  $\alpha_s^n$  in  $p_n$ , this generates the desired  $\alpha_s^n \ln^{n+1} \Lambda^-$  contribution. With the inclusion of virtual emissions, one expects that the modification will be in order of  $\ln \Lambda^- \alpha_s$  as for the  $p_n$ , therefore will not change the leading logarithmic pattern  $\alpha_s^k \ln^{k+1} \Lambda^-$ . Moreover, the leading  $\alpha^k \ln^k \Lambda^-$  and the next to leading  $\alpha^k \ln^{k+1} \Lambda^-$  contributions to the entanglement entropy, can be obtained from the same set of soft gluon LFWFs, that leads to the leading norm-square of the state  $p_n$ . This will be exploited further below.

#### IV. BK-LIKE EVOLUTION OF THE ENTANGLEMENT DENSITY

We now derive an evolution equation for the reduced density matrix in Eq. (16) based on the evolution equation for the dipole generating functional in the large  $N_c$  limit. We first review the derivation of the evolution equation of the dipole's wave function. Since we trace out all the transverse degrees of freedom, and leave only the momentum fractions un-traced, it is more convenient to consider the square of the wave function.

##### A. Evolution of the quarkonium wavefunction

The perturbative process that leads to the leading RD in the dipole's wave function, is by now standard [27, 28, 30]. We briefly recall it here for completeness. The soft

gluons are emitted consecutively with strong ordering in their momentum fractions  $x_1 \gg x_2 \gg x_3 \dots \gg x_n$ . The emission of the first soft gluon at transverse position  $b_2$ , leads the following factor for the wave function square

$$|\Psi^{(1)}|^2 = \int_{x_{\min}}^{x_0} \frac{dx_1}{x_1} \frac{\alpha_s C_F}{\pi^2} \int d^2 b_2 \frac{b_{10}^2}{b_{21}^2 b_{20}^2} |\Psi^{(0)}(b_{10})|^2. \quad (20)$$

Following the emission of the first soft gluon, the original dipole with transverse size  $b_{10}$ , splits into two dipoles with sized  $b_{12}$  and  $b_{20}$ . The subsequent emissions of these two dipoles is independent

$$|\Psi^{(2)}|^2 = \left(\frac{\alpha_s C_F}{\pi^2}\right)^2 \int_{x_{\min}}^{x_0} \frac{dx_1}{x_1} \int_{x_{\min}}^{x_1} \frac{dx_2}{x_2} \int d^2 b_3 \int d^2 b_2 \frac{b_{10}^2}{b_{21}^2 b_{20}^2} \left( \frac{b_{12}^2}{b_{31}^2 b_{21}^2} + \frac{b_{20}^2}{b_{23}^2 b_{30}^2} \right) |\Psi^{(0)}(b_{10})|^2. \quad (21)$$

The process clearly is repetitive, with more and more soft gluons emitted. To generalize to all orders, we define the generating functional  $Z(b_{10}, x_0, u(x, z))$ , such that

$$\frac{1}{n!} \frac{\delta^n Z(b_{10}, x_0, u(b, z))}{\delta u(b_2, z_1) \delta u(b_4, z_2) \dots \delta u(b_{n+1}, x_n)} |\Psi^{(0)}(b_{10})|^2 = |\Psi^{(n)}(b_{10}, x_0; b_2, x_1; b_3, z_2; \dots b_{n+1}, x_n)|^2, \quad (22)$$

Here

$$|\Psi^{(n)}(b_{10}, x_0; b_2, z_1; b_3, z_2; \dots b_{n+1}, z_n)|^2$$

refers to the square of the wave function with  $n$  soft gluons, with transverse positions  $b_2, \dots, b_{n+1}$  and momentum fractions  $x_1 > x_2 > \dots x_n$ . This emission cascade process, satisfies the equation

$$\begin{aligned} Z(b_{10}, x_0, x_{\min}, u) &= S(b_{10}, \frac{x_0}{x_{\min}}) \\ &+ \frac{\alpha_s C_F}{\pi^2} \int_{x_{\min}}^{x_0} \frac{dx_1}{x_1} S(b_{10}, \frac{x_0}{x_1}) \int db_2^2 \frac{b_{10}^2}{b_{12}^2 b_{20}^2} u(x_1, b_2) Z(b_{12}, x_1, x_{\min}, u) Z(b_{20}, x_1, x_{\min}, u). \end{aligned} \quad (23)$$

Here we have included the contribution from virtual emissions that give rise to the Sudakov-like suppression factor

$$S\left(b_{10}, \frac{x_0}{x_1}\right) = \exp\left[-\frac{2\alpha_s C_F}{\pi} \ln b_{10}^2 \mu^2 \ln \frac{x_0}{x_1}\right]. \quad (24)$$

It resums the virtual gluon emissions, prior to the emission of the first real gluon inside the first dipole with size  $b_{10}$ . The constraint that the rapidity of the virtual emission should be between  $x_0$  and the next soft gluon  $x_1$ , leads to the  $\ln \frac{x_0}{x_1}$  contribution. When  $u \equiv 1$ , unitarity requires  $Z = 1$ , which is manifest in the above equation. The evolution equation is depicted in Fig. 1.



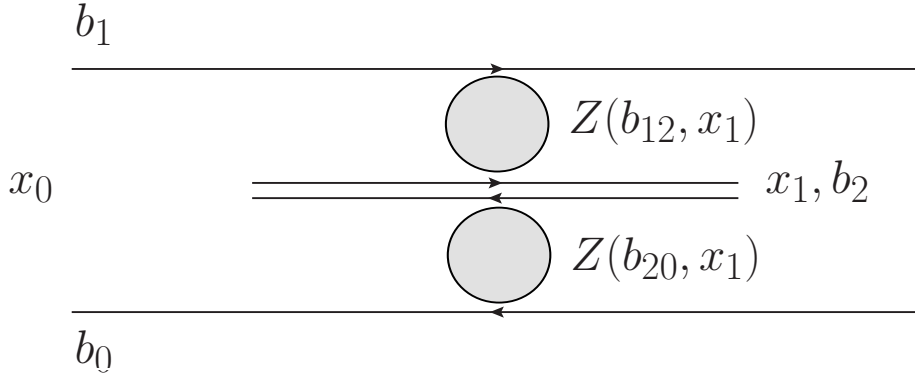


FIG. 1. Depiction of the second term of the evolution equation (23). The first emitted soft gluon at rapidity  $x_1$  and transverse position  $b_2$ , splits the original dipole into two dipoles with transverse separations  $b_{12}$  and  $b_{20}$ , within which subsequent soft emissions occur independently. Virtual emissions before the first real gluon with rapidities between  $x_0$  and  $x_1$ , contribute to the “soft factor”  $S(b_{10}, \frac{x_0}{x_1})$ . When combined with the purely virtual contribution or the first term in (23), unitarity is restored.

### B. Evolution of the density matrix

Given the above, let's consider the reduced density matrix. Clearly, we need all soft gluons in the final states being untraced in rapidity. Since they will be traced in color and in transverse positions, the reduced density should have the same spatial factor as for the squared wave function, except that the momentum fractions on the left-ket and right-bra, are different. Namely, we can have  $x_1 \gg x_2 \gg x_3 \dots \gg x_n$  for the ket and  $x'_1 \gg x'_2 \dots \gg x'_n$  for the bra. However, since the total momentum fraction has to be the same, the largest momentum fractions are approximately equal, namely,  $x_1 \sim x'_1$ . Also, since in the large  $N_c$  limit there is no crossing, we still have the same diagrammatic depiction as in the case of  $Z$ . Moreover, to get the dominant contribution in  $\alpha \ln \Lambda^-$  we expect that the orderings in the bras and kets are one-to-one. Namely, if in the first dipole  $b_{12}$ , the  $k$  soft gluons in kets are labeled by  $x_{\pi(1)}, \dots, x_{\pi(k)}$  where  $\pi$  is a permutation of  $1, 2, \dots, n$ , then in the bras the soft gluons must be  $x'_{\pi(1)}, \dots, x'_{\pi(k)}$ . And similarly for the remaining  $n - k$  soft gluons in the dipole  $b_{20}$ . More precisely, if the wave function reads

$$\begin{aligned}
 & |\bar{Q}Q(b_{10}; x_0, x_{\min})\rangle \\
 &= \sum_n \sum_{x_0 \gg x_1 \gg x_2 \gg x_3 \dots \gg x_n \gg x_{\min}} f_n(b_{10}; x_1, b_1; x_2, b_2; \dots, x_n, b_n) |x_1, b_1\rangle |x_2, b_2\rangle |x_3, b_3\rangle \dots |x_n, b_n\rangle |\bar{Q}\rangle |Q\rangle,
 \end{aligned}
 \tag{25}$$

then with the following *definitions* of the reduced density matrices

$$\begin{aligned} \rho_1(b_{10}; x_0, x'_0, x_{\min}) &= \sum_n \int d^2 b_1 \dots d^2 b_n \\ f_n(b_{10}; x_1, b_1; x_2, b_2; \dots x_n, b_n) f_n^\dagger(b_{10}; x'_1, b_1; x'_2, b_2; \dots x'_n, b_n) &|x_1\rangle|x_2\rangle \dots |x_n\rangle \langle x'_1| \langle x'_2| \dots \langle x'_n|, \end{aligned} \quad (26)$$

and

$$\begin{aligned} \rho(b_{10}; x_0, x_{\min}) &= \sum_n \int d^2 b_1 \dots d^2 b_n \\ f_n(b_{10}; x_1, b_1; x_2, b_2; \dots x_n, b_n) f_n^\dagger(b_{10}; x_1, b_1; x'_2, b_2; \dots x'_n, b_n) &|x_1\rangle|x_2\rangle \dots |x_n\rangle \langle x_1| \langle x'_2| \dots \langle x'_n|, \end{aligned} \quad (27)$$

the locking of the orderings in the bra and ket is automatic in the large  $N_c$  limit. Clearly, this indicates that the soft gluon emissions in the two subsequent dipoles, can be separated from  $x_1, x'_1$  and form two density matrices  $\rho_1(b_{12}, x_1, x_{\min}) \otimes \rho_1(b_{20}, x_1, x_{\min})$ , namely

$$\begin{aligned} \rho_1(b_{10}, x_0, x'_0, x_{\min}, u) &= S^{\frac{1}{2}} \left( b_{10}, \frac{x_0 x'_0}{x_{\min}^2} \right) |0\rangle \langle 0| \\ + \frac{\alpha_s C_F}{\pi^2} \int db_2^2 \frac{b_{10}^2}{b_{12}^2 b_{20}^2} \sum_{x_{\min} \leq x_1, x'_1 \leq x_0} S^{\frac{1}{2}} \left( b_{10}, \frac{x_0 x'_0}{x_1 x'_1} \right) &\frac{|x_1\rangle \langle x'_1|}{\sqrt{x_1 x'_1}} \otimes \rho_1(b_{12}, x_1, x'_1, x_{\min}) \otimes \rho_1(b_{20}, x_1, x'_1, x_{\min}). \end{aligned} \quad (28)$$

And the  $\rho$  can be obtained from  $\rho_1$  by simply tracing the hardest gluon

$$\begin{aligned} \rho(b_{10}, x_0, x_{\min}, u) &= S \left( b_{10}, \frac{x_0}{x_{\min}} \right) |0\rangle \langle 0| \\ + \frac{\alpha_s C_F}{\pi^2} \int db_2^2 \frac{b_{10}^2}{b_{12}^2 b_{20}^2} \sum_{x_{\min} \leq x_1 \leq x_0} S \left( b_{10}, \frac{x_0}{x_1} \right) &\frac{|x_1\rangle \langle x_1|}{x_1} \otimes \rho_1(b_{12}, x_1, x_{\min}) \otimes \rho_1(b_{20}, x_1, x_{\min}). \end{aligned} \quad (29)$$

with  $\rho_1(b, x_1, x_{\min}) \equiv \rho_1(b, x_1, x_1, x_{\min})$ . We note that to order  $\alpha_s$ , the earlier perturbative result can be recovered by expanding the above equations.

Here we should note that both  $\rho(b_{10}, x_0, x_{\min})$  and  $\rho_1(b_{10}, x_0, x_{\min})$  are reduced density matrices.  $\rho_1$  can be viewed as the reduced density matrix of the soft gluon wave function, after tracing over all the degrees of freedom except the rapidity, while  $\rho$  can be obtained from  $\rho_1$  by further tracing out the rapidity of the in-out  $\bar{Q}Q$  pair, which amounts to imposing momentum conservation. (29-28) are the first major results of this paper.

Unfortunately, due to the nature of the kernel in 4D, the structure of the reduced density matrix is complicated for large  $n$ . Below we investigate their entanglement entropies by simplifying the transverse degrees of freedom. We will also show that the partial tracing

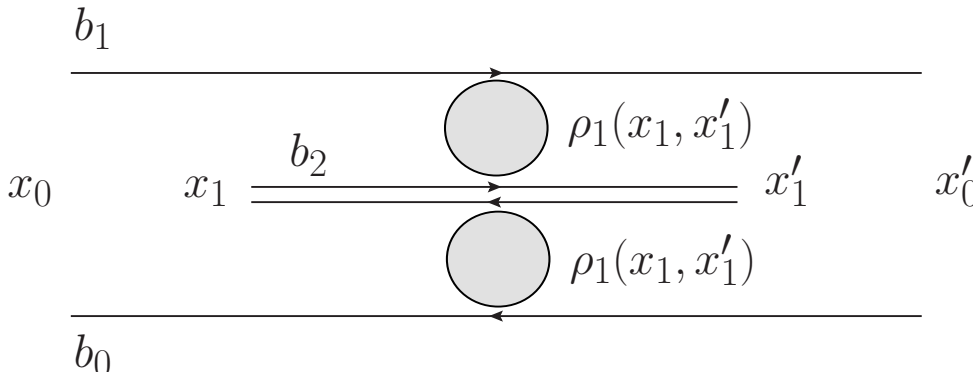


FIG. 2. Depiction of the second term of the evolution equation (28). The first emitted soft gluon at rapidity  $x_1$  and transverse position  $b_2$  splits the original dipole into two dipoles, with transverse separations  $b_{12}$  and  $b_{20}$ , within which subsequent soft emissions forms the corresponding reduced density matrices  $\rho_1(b_{12}, x_1, x'_1)$  and  $\rho_1(b_{20}, x_1, x'_1)$ . Virtual emissions before the first real gluon at left, with rapidities between  $x_0$  and  $x_1$ , contribute to the “soft factor”  $S^{\frac{1}{2}}(b_{10}, \frac{x_0}{x_1})$ , and similarly for  $x'_0, x'_1$  at right. This process should be regarded as the off-diagonal version of the evolution equation (23).

of (28) describes the rapidity evolution of the one-body density matrix, whose eigenvalues and von Neumann entropy are measurable in DIS and hadron-hadron scattering in the diffractive regime. In this spirit, the reduced two-body density following from a pertinent partial tracing of (28), may account for the multiplicities in  $pp$  scattering at the LHC, with two fixed rapidity gaps.

### C. Entanglement entropy in 1+1 reduction

To simplify the analysis of (29-28), we first consider the case where soft emission is solely longitudinal. This amounts to freezing the transverse degrees of freedom, and the resulting evolution equation becomes one dimensional. Note that this is not 2D QCD which is super-renormalizable and with no dynamical gluons. It is more similar to the evolution equation in 4D QCD where the kernel  $\frac{b_{10}^2}{b_{12}^2 b_{20}^2}$  only exhibit moderate decay at large  $b_2$ , but no serious constraint. With this in mind, the 1+1 version of (29-28), is best analysed by following Mueller [28], and by introducing the generating functional with a constant soft gluon current  $u$

$$Z(y, u) = e^{-ay} + au e^{-ay} \int_0^y e^{ay_1} dy_1 Z(y_1, u) Z(y_1, u). \quad (30)$$

We have identified the rapidity of the  $\bar{Q}Q$  pair with  $y$

$$y = \ln \frac{x_0}{x_{\min}} = \ln x_0 \Lambda^- . \quad (31)$$

and reduced the Sudakov factor (24) to  $e^{-ay}$ , by assuming  $b$ -independence

$$\frac{2\alpha_s C_F}{\pi} \ln b_{10}^2 \mu^2 \rightarrow a \quad (32)$$

The above equation can be easily solved by iterating Eq. (30)

$$Z(y, u) = \sum_{n=0}^{\infty} e^{-ay} u^n \left(1 - e^{-ay}\right)^n, \quad (33)$$

with  $Z(y, 1) = 1$ . From the above, we can read the probability of finding  $n$  soft gluons as

$$p_n = e^{-ay} \left(1 - e^{-ay}\right)^n = \frac{1}{\bar{n} + 1} \left(1 - \frac{1}{\bar{n} + 1}\right)^n \quad (34)$$

with  $\bar{n} = \sum_n n p_n = e^{ay} - 1$  the mean number. As noted in [28], we have  $\bar{n} p_n \approx e^{-n/\bar{n}}$  for large mean  $\bar{n}$ , in agreement with KNO scaling.

### Density matrices:

The reduced density matrix for the untraced soft gluons *without* overall momentum conservation is

$$\hat{\rho}_1 = \sum_{n=0}^{\infty} |\Psi_n\rangle \langle \Psi_n|, \quad (35)$$

with the effective state

$$|\Psi_n\rangle = \sum_{x_0 \gg x_1 \gg x_2 \dots \gg x_n \gg x_{\min}} \sqrt{a^n n!} \frac{e^{-\frac{ay+a \sum_{i=1}^n y_i}{2}}}{\sqrt{(\Lambda^-)^n x_1 \dots x_n}} |x_1\rangle |x_2\rangle \dots |x_n\rangle, \quad (36)$$

where  $y_i = \ln \frac{x_i}{x_{\min}}$ . Notice that for each  $n$ ,  $\rho_1$  is already in the diagonal form, therefore it is the full reduced density matrix without assumptions in the ordering of  $x_1, x_2, \dots, x'_n$ . In contrast, the one *with* momentum conservation is

$$\rho = \sum_n \sum_{x_1} |\Psi_{x_1, n}\rangle \langle \Psi_{x_1, n}|, \quad (37)$$

with the state

$$|\Psi_{x_1, n}\rangle = \frac{e^{-\frac{ay_1}{2}}}{\sqrt{\Lambda^- x_1}} |x_1\rangle \sum_{x_1 \gg x_2 \dots \gg x_n \gg x_{\min}} \sqrt{a^n n!} \frac{e^{-\frac{ay+a \sum_{i=1}^n y_i}{2}}}{\sqrt{(\Lambda^-)^{n-1} x_2 \dots x_n}} |x_2\rangle \dots |x_n\rangle. \quad (38)$$

Both reduced density matrices satisfy the BK-like evolution equations (29-28)

### Entanglement entropy from $\hat{\rho}_1$ :

The entanglement entropy associated to  $\rho_1$ , for the soft gluon wave function without the

overall momentum constraint (with the longitudinal momentum of the  $\bar{Q}Q$  untraced), is readily obtained using the von Neumann entropy and the gluon probabilities (34)

$$S(\hat{\rho}_1) = - \sum_{n=0}^{\infty} p_n \ln p_n = ay - \ln(1 - e^{-ay}) \left( e^{ay} - 1 \right) \rightarrow ay + 1 + \mathcal{O}(e^{-ay}) , \quad (39)$$

It asymptotes  $ay$  for large rapidity  $y \rightarrow \infty$ , with  $a \sim \alpha_s C_F$ . This result was noted when analysing DIS scattering at weak coupling in the Regge limit [16], and hadron-hadron scattering also in the Regge limit at strong coupling in [15] (although in the latter it was initially identified as a quantum entropy).

In the Regge limit, DIS and hadron-hadron scattering are universally described by dipole-dipole scattering [28]. In weak coupling, the scattering is dominated by exchange of BFKL pomerons. At strong coupling, the scattering is dominated by closed string exchanges. The entanglement entropy controls the rise of the low- $x$  gluons in DIS, and the rise of the large- $s$  elastic cross section in diffractive hadron-hadron scattering.

The eigenvalues  $p_n$  of the reduced density matrix  $\hat{\rho}_1$ , describe the wee parton multiplicities at low- $x$  or large  $\sqrt{s}$ , that may turn real in an inclusive DIS process, or a diffractive hadronic process with particle production, and KNO scaling. In this sense, the entanglement content of the reduced density matrix  $\hat{\rho}_1$ , with untraced or fixed  $\bar{Q}Q$  longitudinal momenta, is directly accessible to DIS, or hadron-hadron scattering in the Regge limit. In Nuclei, an even larger form of entanglement maybe at work, as we suggested recently [22].

### Entanglement entropy from $\hat{\rho}$ :

The reduced density matrix  $\hat{\rho}$  after tracing the  $\bar{Q}Q$  is expected to be more entangled, with a larger entanglement entropy. Indeed, the entanglement entropy is now of the form

$$S(\rho) = aye^{-ay} - \sum_{n=1}^{\infty} \int_0^y dy_1 \ln \left[ nae^{-a(y+y_1)-y_1} (1 - e^{-ay_1})^{n-1} \right] nae^{-a(y+y_1)} (1 - e^{-ay_1})^{n-1} . \quad (40)$$

To evaluate (40) we split it into three contributions

$$\begin{aligned} S(\rho) - aye^{-ay} &= \sum_{n=1}^{\infty} \int_0^y dy_1 \left( y_1 + a(y + y_1) \right) nae^{-a(y+y_1)} (1 - e^{-ay_1})^{n-1} \\ &- \sum_{n=0}^{\infty} \ln(na) p_n - \sum_{n=0}^{\infty} \int_0^y dy_1 \ln(1 - e^{-ay_1}) n(n-1) ae^{-a(y+y_1)} (1 - e^{-ay_1})^{n-1} . \end{aligned} \quad (41)$$

The first contribution in (40) can be calculated by summing over  $n$

$$\begin{aligned} S_1 &= \sum_{n=1}^{\infty} \int_0^y dy_1 \left( y_1 + a(y + y_1) \right) nae^{-a(y+y_1)} (1 - e^{-ay_1})^{n-1} \\ &= \int_0^y dy_1 a \left[ y_1 + a(y + y_1) \right] e^{-a(y-y_1)} = y(1 + 2a) - \frac{1+a}{a} + \mathcal{O}(e^{-ay}) , \end{aligned} \quad (42)$$

and then expanding for large rapidity  $y$ . Similarly, the third contribution in (40) gives

$$\begin{aligned} S_3 &= - \sum_{n=1}^{\infty} \int_0^y dy_1 \ln(1 - e^{-ay_1}) n(n-1) a e^{-a(y+y_1)} (1 - e^{-ay_1})^{n-1} \\ &= - 2e^{-ay} \int_0^y a dy_1 \ln(1 - e^{-ay_1}) (1 - e^{-ay_1}) e^{2ay_1} . \end{aligned} \quad (43)$$

By using the inequality

$$-\ln(1 - e^{-ay_1})(1 - e^{-ay_1}) \leq e^{-ay_1} , \quad (44)$$

we have

$$S_3 \leq 2(1 - e^{-ay}) . \quad (45)$$

On the other hand, using the inequality  $-\ln(1 - e^{-ay_1}) \geq e^{-ay_1}$ , we also have

$$S_3 \geq 2(1 - e^{-ay}) - 2ay e^{-ay} . \quad (46)$$

Thus, as  $y \rightarrow \infty$  we have

$$S_3 \rightarrow 2 + \mathcal{O}(y e^{-ay}) . \quad (47)$$

Finally, the second contribution in (40) can be calculated for large  $y$  as

$$S_2 = - \sum_{n=0}^{\infty} \ln(na) p_n \rightarrow -ay - \ln a - \int_0^{\infty} dx \ln x e^{-x} = -ay - \ln a + \gamma_E . \quad (48)$$

Given the above, we found that the non-vanishing part of the entanglement entropy reads

$$S(\rho) = y(1+a) + 1 + \gamma_E - \frac{1}{a} - \ln a = \ln(x_0 \Lambda^-)(1+a) + 1 + \gamma_E - \frac{1}{a} - \ln a . \quad (49)$$

with  $\gamma_E$  being the Euler constant.

In sum, to any given order in  $a$ , each soft emission, either real or virtual, is accompanied by a  $y^n$  divergence in the wavefunction, at order  $a \sim \alpha_s C_F$  and large rapidity  $y$ . However, the re-summed divergences to order  $ay$  are finite and saturate the Kolmogorov-Sinai bound of 1. The bound was noted in [22]. The entanglement entropy remains linear in  $y$ , despite the growing rapidity divergences with increasing order in  $\alpha_s$ .

#### D. Entanglement entropies and saturation in 3D QCD

DIS or hadron-hadron scattering in 3D QCD which is super-renormalizable, non-conformal and confining, is still dominated by soft gluon emissions at weak coupling in the Regge limit. The BK-like equations for the corresponding density matrices (29-28) still

hold. Interestingly, this case can be solved exactly with both longitudinal and transverse evolution in place.

Indeed, in 3D the BK-like evolution equations can be solved using the generating functional

$$Z(b, y, u) = e^{-mb y} + u m \int_0^y dy_1 e^{-mb(y-y_1)} \int_0^{b'} db' Z(b-b', y_1, u) Z(b', y_1, u), \quad (50)$$

with  $m \equiv \frac{g_{1+2}^2 C_F}{4\pi^2}$  the mass scale in 3D. To derive this equation, we start with (6), and write it in coordinate space. Using the identity

$$\int_{-\infty}^{\infty} \frac{dk^z}{(2\pi)} \frac{e^{ik^z b}}{k^z} = \frac{i}{\pi} \int_0^{\infty} \frac{dk^z}{k^z} \sin(k^z b) = \frac{i}{2} \text{sign}(b), \quad (51)$$

we now have the wave function in the coordinate space, after the emission of a single soft gluon

$$\begin{aligned} \Psi^a(x, z, b_1, b_0, b_2, \epsilon) &= \int \frac{dk_{\perp} dk_{g,\perp}}{(2\pi)^2} e^{ikb_{10} + k_g b_{20}} \Psi^a(x, z, k, k_g, \epsilon) \\ &= \frac{igt^a}{2\pi\sqrt{x}} \Psi^0(z, b_1)_{\sigma,\sigma'} \epsilon \left( \text{sign}(b_{21}) - \text{sign}(b_{20}) \right). \end{aligned} \quad (52)$$

This means that the emitted gluon position  $b_2$  lies between the mother dipole positions 0 and 1, in transverse space and consequently the integral over  $b_2$  is IR safe. Given the above, the derivation of the evolution equation is identical to the 4D case which yields (50) with  $m = \frac{\alpha_s C_F}{\pi}$ .

It is not hard to show that the solution of the equation above can be solved explicitly. First, the generating functional can be shown to be

$$Z(b, y, u) = e^{-mb y} \sum_{n=0}^{\infty} u^n \frac{(mb y)^n}{n!} = e^{mb y(u-1)}. \quad (53)$$

Indeed, when plugged into (50), one can readily verify that the above is indeed the solution with the condition  $Z(b, y, 1) = 1$ . From these, one identifies the probability of finding  $n+1$  dipoles with the Poisson gluon emissivities

$$p_n = e^{-mb y} \frac{(mb y)^n}{n!}. \quad (54)$$

The reduced density matrix without the momentum constraint can be shown to be

$$\hat{\rho}_1 = \sum_n \hat{\rho}_{1,n} = \sum_{x_1 \gg x_2 \dots \gg x_n, x'_1 \gg x'_2 \dots \gg x'_n} \frac{e^{-mb y} (mb)^n}{(\Lambda^-)^n \sqrt{x_1 x_2 \dots x_n x'_1 x'_2 \dots x'_n}} |x_1 \dots x_n\rangle \langle x'_1 \dots x'_n|, \quad (55)$$

from which one reads the most singular part of the x-weighted gluon PDF as

$$xf_g(x) = mbx^{mb} , \quad (56)$$

which as expected, is independent of  $y$  or RD free. (56) is the gluonic structure function, which is usually accessible to DIS kinematics in the Regge limit.

Given  $\rho_1$ , the corresponding density matrix with the momentum constraint  $\hat{\rho}$  follows from  $\hat{\rho}_1$  by setting  $x_1 = x'_1$ . The von Neumann entropy for  $\hat{\rho}_1$  is

$$S(\rho_1) = - \sum_n p_n \ln p_n , \quad (57)$$

while for  $\hat{\rho}$

$$S(\rho) = -p_0 \ln p_0 - \sum_{n=1}^{\infty} \int dy_1 \frac{y_1^{n-1} (mb)^n e^{-mby}}{(n-1)!} \ln \left( \frac{y_1^{n-1} (mb)^n e^{-mby}}{(n-1)!} e^{-y_1} \right) , \quad (58)$$

At large  $b$ , the latter is extensive in  $y$ . Indeed, using the Stirling's formula

$$\sqrt{2\pi n} \left( \frac{n}{e} \right)^n e^{\frac{1}{12n+1}} < n! < \sqrt{2\pi n} \left( \frac{n}{e} \right)^n e^{\frac{1}{12n}} , \quad (59)$$

we can simplify the integrand in (58)

$$\sum_{n=1}^{\infty} \frac{(mby)^n}{n!} e^{-mby} n \ln n \rightarrow mby \ln(mby) - mby + \frac{1}{2} \ln mby + \frac{1}{2} \ln 2\pi + \frac{1}{2} . \quad (60)$$

The first term follows from the peak of the Poisson distribution, but the next contributions require the full formula. Inserting (60) in (57) we obtain for the entanglement entropies

$$\begin{aligned} S(\rho_1) &\rightarrow \frac{1}{2} \ln(2\pi emb y) , \\ S(\rho) &\rightarrow y + \frac{1}{2} \ln(2\pi emb y) + 1 . \end{aligned} \quad (61)$$

Unlike 4D QCD, the entanglement entropy for  $\hat{\rho}_1$  in the non-conformal 3D QCD, is not extensive in the rapidity  $y$ . The rate of growth of the entropy vanishes at large rapidities, a result which is consistent with the lack of growth of the gluonic structure function in (56). This kinematical form of *saturation* is a consequence of the specific form of the evolution kernel: in 3D QCD, the transverse position  $b_2$  of the emitted dipole is forced to be *within* the original dipole as in (50). Therefore, when there are more and more dipoles in the wave function, the average size for these dipoles will become smaller and smaller, and the probability for emitting new dipoles will be penalized. This is not the case in 4D where the emission of new dipoles with large sizes is not penalized strongly.

Finally, we note that the entanglement entropy for  $\hat{\rho}$ , is similar to that for  $\hat{\rho}_1$  plus an additional linear contribution in  $y$ . This extensivity in  $y$  follows from the extra tracing over the  $\bar{Q}Q$  pair, and in-out longitudinal momentum conservation.



## V. EMERGENT ADS SPACE FROM RAPIDITY EVOLUTION IN QCD

The integral equations for the density matrices in (29-28), reflect on the multi-body content of the soft emissions in the  $\bar{Q}Q$  state. They are part of the contributions in onium-onium (dipole-dipole) scattering, as originally discussed by Mueller [27, 28]. A more general reduced matrix that is off-diagonal in both the rapidity and the dipole size can be inferred from (26), by substituting  $b_1 \rightarrow b'_1$  in the outgoing amplitude  $f^\dagger$  without tracing over  $b_1$ . After performing the partial traces of this entangled density matrix, we obtain the BFKL evolution for the so-called dipole-dipole Green's function. In the process, we will unravel an emergent AdS structure that will allow us to bridge the perturbative or partonic contribution for soft gluon emissivities, with the non-perturbative string contribution using string bits.

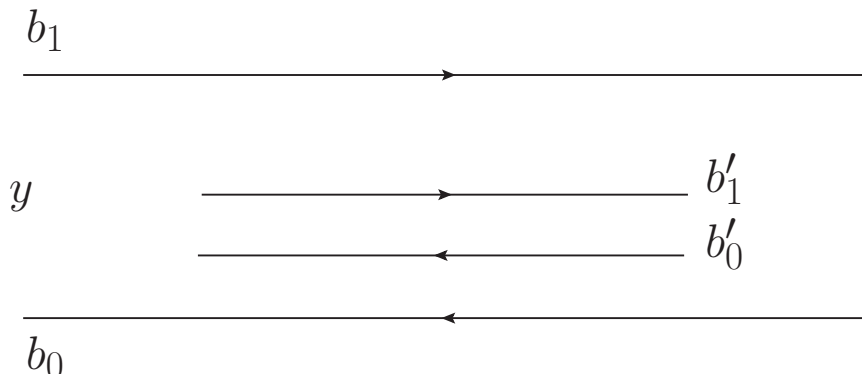


FIG. 3. Illustration of the dipole-dipole correlation function  $n(b_{10}, b_{10}, b, y)$ :  $b_{10} = b_1 - b_0$  is the size of the mother dipole, and  $b'_{10} = b'_1 - b'_0$  the size of the daughter dipole. The impact parameter is given by  $b = \frac{b'_0 + b'_1}{2} - \frac{b_1 + b_0}{2}$

With this in mind, we introduce the *dipole-dipole Green's function*  $n(b_{10}, b'_{10}, b, y)$ , defined as the probability of finding a *daughter* dipole with size  $b'_{10}$  and at impact parameter  $b$ , within the wave function of the *mother* dipole  $b_{10}$ ,

$$n(b_{10}, b'_{10}, b, y) = \frac{\delta \tilde{Z}(b_{10}, b_0, x_0, x_{\min}, J)}{\delta J(b + b_0, b'_{10})} \Big|_{J=1}, \quad (62)$$

where

$$\begin{aligned} \tilde{Z}(b_{10}, b_0, x_0, x_{\min}, J) &= S(b_{10}, b_0, \frac{x_0}{x_{\min}}) J(b_0, b_{10}) \\ &+ \frac{\alpha_s C_F}{\pi^2} \int_{x_{\min}}^{x_0} \frac{dx_1}{x_1} S(b_{10}, \frac{x_0}{x_1}) \int db_2^2 \frac{b_{10}^2}{b_{12}^2 b_{20}^2} \tilde{Z}(b_0 - \frac{b_{20}}{2}, b_{12}, x_1, x_{\min}, J) \tilde{Z}(b_0 + \frac{b_{12}}{2}, b_{20}, x_1, x_{\min}, J). \end{aligned} \quad (63)$$

is the generating functional for the dipole wave function squares. The dipole current  $J(b, b_{12})$  refers to a dipole of transverse size  $b_{12}$  centered at  $b$  as illustrated in Fig. 3. It follows that  $n$  satisfies the evolution equation in rapidity

$$\begin{aligned} \partial_y n(b_{10}, b'_{10}, b, y) &= \frac{\alpha_s N_c}{2\pi^2} \int d^2 b_2 \frac{b_{10}^2}{b_{12}^2 b_{20}^2} \\ &\left[ n(b_{12}, b'_{10}, b - \frac{b_{20}}{2}, y) + n(b_{20}, b'_{10}, b - \frac{b_{21}}{2}, y) - n(b_{10}, b'_{10}, b, y) \right]. \end{aligned} \quad (64)$$

This equation has an  $SL(2, C)$  symmetry [9, 30], which is more transparent in the holomorphic coordinates  $\rho_i = x_i + iy_i$ , where  $b_i = (x_i, y_i)$  are the transverse positions of the four boundaries  $b_0, b_1, b'_0, b'_1$  of the two dipoles, with  $b_{10} = b_1 - b_0$  and  $b'_{10} = b'_1 - b'_0$ . In these coordinates, the BFKL equation becomes

$$\partial_y n(\rho_1, \rho_0; \rho'_1, \rho'_0; y) = \frac{\alpha_s N_c}{2\pi^2} \left( H_{GG} + \bar{H}_{GG} \right) n. \quad (65)$$

The BFKL Hamiltonian can be written in terms of the generator of  $SL(2, C)$  [9, 31, 32]

$$M^z = \rho_1 \partial_1 + \rho_2 \partial_2, \quad M^+ = -\rho_1^2 \partial_1 - \rho_2^2 \partial_2, \quad M^- = \partial_1 + \partial_2, \quad (66)$$

and its Casimir operator

$$M^2 = (M^z)^2 - \frac{1}{2}(M^+ M^- + M^- M^+) = -\rho_{12}^2 \partial_1 \partial_2, \quad (67)$$

as

$$H_{GG} = \sum_{l=0}^{\infty} \left( \frac{2l+1}{l(l+1) - M^2} - \frac{2}{l+1} \right). \quad (68)$$

The same applies to the anti-holomorphic section. The eigenvalues of the Casimir depend on  $n \in Z$  and  $\nu \in R$ ,

$$-M^2 E_{n,\nu} = h(h-1) E_{n,\nu}, \quad -\bar{M}^2 E_{n,\nu} = \bar{h}(\bar{h}-1) E_{n,\nu}, \quad (69)$$

with specifically

$$h = \frac{1+n}{2} + i\nu, \quad \bar{h} = \frac{1-n}{2} - i\nu. \quad (70)$$

and the eigenvalues

$$E_{n,\nu}(\rho_{1a}, \rho_{2a}) = \left( \frac{\rho_{12}}{\rho_{1a}\rho_{2a}} \right)^h \left( \frac{\bar{\rho}_{12}}{\bar{\rho}_{1a}\bar{\rho}_{2a}} \right)^{\bar{h}}, \quad (71)$$

In terms of these, it is easy to see that the eigenvalues of  $H + \bar{H}$  are real, equal and given by the di-gamma function

$$\chi(n, \nu) = 4\text{Re}\psi\left(\frac{1+|n|}{2} + i\nu\right) - 4\psi(1). \quad (72)$$

With this in mind, the solution for the reduced dipole density  $n$  in (65), can be written in terms of the eigenfunctions of the BFKL Hamiltonian and its holomorphic section,

$$n(\rho_1, \rho_0, \rho'_1, \rho'_0) = \sum_n \int_{-\infty}^{\infty} d\nu C_{n,\nu} e^{y\bar{\alpha}_s \chi(n,\nu)} \int d^2 \rho_a E_{n,\nu}(\rho_{1a}, \rho_{0a}) E_{n,\nu}(\rho_{1'a}, \rho_{2'a}) , \quad (73)$$

We now note that the integrand in (73) can be re-written in terms of hyper-geometrical functions, using the conformal variable [9, 30]

$$w = \frac{\rho_{10}\rho_{1'0'}}{\rho_{11'}\rho_{00'}} , \quad (74)$$

as

$$\begin{aligned} G_{n\nu}(\rho_1, \rho_0, \rho'_1, \rho'_0) &= c_1 x^h \bar{x}^{\bar{h}} F[h, h, 2h, x] F[\bar{h}, \bar{h}, 2\bar{h}, \bar{x}] \\ &+ c_2 x^{1-h} \bar{x}^{1-\bar{h}} F[1-h, 1-h, 2(1-h), x] F[1-\bar{h}, 1-\bar{h}, 2(1-\bar{h}), \bar{x}] . \end{aligned} \quad (75)$$

Remarkably,

$$x^h F[h, h, 2h, x] , \quad (76)$$

is the scalar propagator in conformal AdS<sub>3</sub> space (identified as  $1_y + 1_b + 1_z$ ), with the invariant AdS<sub>3</sub> length

$$x \sim \frac{zz'}{(z-z')^2 + (b-b')^2} .$$

In our case, the transverse  $b$  is large with  $x \sim \frac{uu'}{b^2}$ . In this limit, (73) is dominated by the ground state with  $n = 0$ ,

$$\frac{b_{10}b'_{10}}{b^2} \int d\nu C_{0,\nu} c_1(0, \nu) \left( \frac{b_{10}b'_{10}}{b^2} \right)^{2i\nu} e^{y\bar{\alpha}_s \chi(0,\nu)} . \quad (77)$$

with the lowest eigenvalue

$$\chi(0, \nu) \sim 4 \ln 2 - 14\zeta_3 \nu^2 , \quad (78)$$

The result is a Gaussian integral, which always gives a factor

$$\exp \left[ 4 \ln 2 \bar{\alpha}_s y - \frac{\pi}{14\alpha\zeta_3 N_c y} \ln^2 \frac{b^2}{b_{10}b'_{10}} \right] , \quad (79)$$

The pre-factor depends on the initial condition. For large  $b$ , one can identify  $(M^z)^2$  with the Laplacian in AdS<sub>3</sub>,

$$z^2 (\partial_z^2 + \partial_b^2) f \left( \frac{zz'}{b^2} \right) \rightarrow \frac{z^2 (z')^2}{b^4} f'' \left( \frac{zz'}{b^2} \right) , \quad (80)$$

$$-\rho_{12}^2 \partial_1 \partial_2 f \left( \frac{\rho_{12}\rho'_{12}}{b^2} \right) \rightarrow \frac{\rho_{12}^2 (\rho'_{12})^2}{b^4} f'' \left( \frac{\rho_{12}\rho'_{12}}{b^2} \right) . \quad (81)$$

This explains the match in the eigenfunctions. Note that in AdS<sub>3</sub>, the eigenvalues for the scalar field are

$$i\Delta = \sqrt{-M^2 + E}, \quad E = M^2 - \Delta^2, \quad (82)$$

which match those of the BFKL kernel. Therefore, at large  $b$  there is an emergent AdS<sub>3</sub> structure of the BFKL solution. The propagator, the Laplacian and the symmetry match.

To explain the pre-factor, requires the initial condition. Specifically, for the initial condition

$$n(b_{10}, b_{1'0'}, b, y = 0) = \frac{2\alpha_s C_F}{N_c} \ln^2 \frac{b_{11'} b_{00'}}{b_{10'} b_{01'}}, \quad (83)$$

we fix the expansion coefficient  $C_{n,\nu}$  in (73) as

$$C_{n,\nu} = \frac{\nu^2 + \frac{n^2}{4}}{\left(\nu^2 + \frac{(n-1)^2}{4}\right) \left(\nu^2 + \frac{(n+1)^2}{4}\right)} \Gamma\left(\frac{|n|}{2} + i\nu\right) \times \tilde{C}, \quad (84)$$

For  $n = 0$ , it behaves as  $i\nu$  for small  $\nu$ , and is dominant in the large  $b$ , or large  $y$  limits. This leads the additional contribution

$$\ln\left(\frac{b^2}{b_{10} b'_{10}}\right) \frac{1}{y}, \quad (85)$$

When combined with the factor of  $1/y^{\frac{1}{2}}$  from the gaussian integral, this yields the expected rapidity dependent pre-factor  $1/y^{\frac{3}{2}}$ !

## VI. STRING DUAL DESCRIPTION OF RAPIDITY EVOLUTION IN ADS SPACE

The emergence of an AdS space structure that characterizes Mueller dipole evolution [27, 28] in rapidity in the BFKL limit, is purely in the perturbative realm of QCD. This is not totally surprising, since the BFKL equation exhibit conformal symmetry. Yet this relationship is useful, as it points to the string dual description in AdS space at strong coupling [33–38]. Indeed, Feynman wee-parton description (weak coupling) [6], is dual to Susskind-Thorn string-bit description [13, 14] (strong coupling), albeit in curved AdS space. This allows for the extension of the entanglement entropy calculations at weak coupling [16], to strong coupling and large  $N_c$ , as originally suggested in the form of a quantum entropy in the context of holography [15].

In the AdS approach, the holographic direction  $z$  is dual to the dipole sizes  $x_{10}, x'_{10}$ , and the impact parameter space can be of arbitrary  $d_{\perp}$  dimensions [35, 36]. The relevant

quantity is the tachyon propagator [15]

$$G(\Delta(j), W) = W^\Delta F[\Delta(j), \Delta(j) + \frac{1-d_\perp}{2}, 2\Delta(j) + 1 - d_\perp, -4W] , \quad (86)$$

which can be naturally expressed in the invariant AdS length

$$W = \frac{zz'}{(z-z')^2 + b^2} , \quad (87)$$

Here  $\Delta(j)$  is related to the string tachyon mass  $M_0^2 = -(d_\perp + 1)/6\alpha'$  ( $\alpha' \sim 1/\sqrt{\lambda}$  is the squared string length in units of the AdS radius), through the relation

$$\Delta(j) = \frac{d_\perp}{2} + \sqrt{-M_0^2 - j - \frac{d_\perp^2}{4}} . \quad (88)$$

The Green-function can be written in this case as

$$N(T_\perp, zz'/b^2) \sim \int dj e^{jT_\perp} G(\Delta(j), W) . \quad (89)$$

If we identify  $\Delta(j)$  with the weight in the BFKL kernel

$$h = \frac{1}{2} + i\nu , \quad (90)$$

we find that  $d_\perp = 1$ , and the variable conjugate to  $y = \frac{T_\perp}{\mathcal{D}}$  as

$$\mathcal{E} = \mathcal{D}j = \mathcal{D} \left( -M_0^2 - \frac{d_\perp^2}{4} - \nu^2 \right) , \quad (91)$$

with  $\mathcal{D} = \alpha'/2$ , and therefore

$$\alpha_{\mathbb{P}} = \mathcal{D} \left( -M_0^2 - \frac{d_\perp^2}{4} \right) = \frac{\alpha'}{2} \left( \frac{d_\perp + 1}{6\alpha'} - \frac{d_\perp^2}{4} \right) . \quad (92)$$

with  $\alpha_{\mathbb{P}}$  the Pomeron intercept. Since  $M_0^2 \propto -\frac{1}{\alpha'}$  and  $\mathcal{D} \propto \alpha'$ , the dominant contribution clearly comes from the tachyon mass  $-M_0^2$ . Similarly, in the BFKL case the conjugate variable to  $y$  reads

$$\mathcal{E} = \bar{\alpha}_s \left( 4 \ln 2 - 14\zeta_3 \nu^2 \right) , \quad (93)$$

from which one has the standard

$$\alpha_{\text{BFKL}} = 4 \ln 2 \bar{\alpha}_s , \quad \mathcal{D}_{\text{BFKL}} = 14\zeta_3 \bar{\alpha}_s , \quad (94)$$

with  $\bar{\alpha}_s = \frac{\alpha_s N_c}{\pi}$ .

Alternatively, we may identify the tachyon propagator (89), with the BFKL integral

$$\int d\nu\nu \left( \frac{b_{10}b'_{10}}{b^2} \right)^{1+2i\nu} e^{\bar{\alpha}_s(4\ln 2 - 14\zeta_3\nu^2)}, \quad (95)$$

More specifically, the BFKL parameters are now

$$h + \bar{h} = 1 + 2i\nu = \frac{d_\perp}{2} + \sqrt{-M_0^2 - j - \frac{d_\perp^2}{4}}, \quad (96)$$

with

$$\alpha_{\text{BFKL}} = 4\ln 2\bar{\alpha}_s, \quad \mathcal{D}_{\text{BFKL}} = \frac{7}{2}\zeta_3\bar{\alpha}_s, \quad (97)$$

replacing the identification (94). This implies that the emergent AdS transverse dimensionality is  $D_\perp = d_\perp + 1_z = 3$ , leading to  $\text{AdS}_{2+3=5}$ . The ensuing BFKL evolution is instead in an emergent  $\text{AdS}_5$ , which is the identification made in [39]. Namely, the relevant structure in the BFKL side is a product of two hyper-geometric functions, with the doubling of the pre-factors  $\frac{zz'}{b^2}$ .

### Entanglement entropy and multiplicities at strong coupling:

The string dual reduced entanglement density matrix in  $1 + 1 + D_\perp$  dimensions, can be derived explicitly for long strings in the confining regime. Remarkably, its spectrum is dominated by the collective eigenvalues [40]

$$p_n(D_\perp) = \frac{(n + D_\perp - 1)!}{n!D_\perp!} e^{-\frac{D_\perp}{6}y} \left( 1 - e^{-\frac{1}{6}y} \right)^n, \quad (98)$$

which generalize (34) to arbitrary  $D_\perp$ , at strong coupling and large  $N_c$ . The remaining eigenvalues are small, and randomly (Poisson) distributed. The normalized q-moments of (98) are captured by a PolyLog

$$C(q) = \frac{\langle n^q \rangle}{\langle n \rangle^q} = \frac{1}{\langle n \rangle^q (\langle n \rangle - 1)} \text{PolyLog} \left( -q, 1 - \frac{1}{\langle n \rangle} \right), \quad (99)$$

with the mean multiplicity

$$\langle n \rangle = D_\perp e^{\frac{y}{6}} \rightarrow D_\perp \left( \frac{s}{s_0} \right)^{\frac{1}{6}}. \quad (100)$$

The rightmost relation follows from the identification of the rapidity  $y = \ln \frac{s}{s_0}$ , for hadron-hadron scattering at large  $\sqrt{s}$ . In Fig. 4, we compare the multiplicity moments extracted from  $pp$  scattering at LHC at  $\sqrt{s} = 7$  TeV in the pseudo-rapidity interval  $\eta \leq 0.5$  [41] as

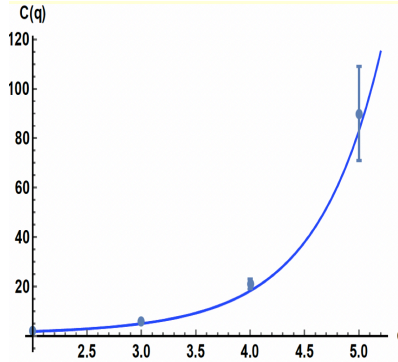


FIG. 4. Multiplicity moments extracted from  $pp$  scattering at LHC at  $\sqrt{s} = 7$  TeV in the pseudo-rapidity interval  $\eta \leq 0.5$  [41] as quoted in [16], versus the Polylog function following from the dual string analysis in (99).

quoted in [16], versus the moments  $C(q)$  in (99) shown through the continuous q-Polylog. The entanglement entropy is saturated by the collective eigenvalues of the string (98)

$$-\sum_n p_n(D_\perp) \ln p_n(D_\perp) \approx \frac{D_\perp}{6} y \rightarrow 2\alpha_{\mathbb{P}} y \quad (101)$$

with the rightmost result following from (92) [15] (Note the difference of 1 in the definition of the Pomeron intercept in [15]). A similar result was noted in [42], using a spin-chain analysis [9]. In diffractive  $pp$  and DIS scattering, the entanglement entropy is captured by twice the Pomeron intercept, and therefore *measurable!* As we noted earlier, the additional partial tracing of (28), may account for possible multiplicities with double rapidity gaps also in the diffractive regime, and may be accessible in current  $pp$  collisions at the LHC.

Finally, the correspondence with a string in  $\text{AdS}_5$ , allows the identification of an Unruh-like temperature  $T = (y/b)/2\pi$ , on the string world-sheet at large rapidity  $y$ , and large  $b$  with a wall to account for confinement [37]. As a result, the effective thermal entropy associated to the string using standard thermodynamics (derivative of the string classical free energy) at large rapidity [15, 40], is found to match the quantum string entanglement entropy (101). This extends the concept of entanglement induced by small- $x$  radiation in quarkonium at weak coupling  $\alpha_s$  and large  $N_c$ , to strong 't Hooft coupling  $\lambda = g_s^2 N_c$  and large  $N_c$  in walled  $\text{AdS}_5$  (a dual of confining QCD).

## VII. CONCLUSIONS

Hadrons undergoing large boosts are surrounded by ever-growing wee parton clouds. In perturbative QCD, this growth is dominated by soft gluon emission. This growth is captured by the entanglement content of the hadronic wavefunction, with the quarkonium wavefunction being the simplest illustrative example of this phenomenon.

We have explicitly constructed the quarkonium wavefunction on the light front at leading order in  $\alpha_s$ , by including both the real and virtual contributions. The entanglement entropy from the real emission is found to be of order  $\alpha_s y^2$ , in comparison to the virtual emission which is of order  $\alpha_s y$ . This enhancement is shown to propagate to higher orders, with a contribution of order  $\alpha_s^n y^{n+1}$  to the entanglement entropy.

In the large  $N_c$  limit and weak gauge coupling, the leading density matrix of quarkonium, obtained by tracing over a single longitudinal cut  $[x_{\min}, x_0]$ , can be re-summed in a closed form. The reduced density matrices with and without overall longitudinal momentum conservation, are shown to obey non-local BK-like integral equations for QCD in any space-time dimension larger than 2, as there is no radiative gluons in 2D. (They may generalize to strong gauge coupling, using the arguments in [43]).

We solve these equations for QCD in 4D with only longitudinal evolution, and non-conformal QCD in 3D including both transverse and longitudinal evolution. For the former, the entanglement entropy is found to be at the Kolmogorov-Sinai bound of 1, when the in-out longitudinal momenta are fixed. For the latter, the rate of change of the entanglement entropy is found to vanish at large rapidities, since the soft gluon multiplication is limited by a narrowing transverse space.

The rapidity evolution of the trace of the reduced density matrix without longitudinal momentum conservation, obeys a diffusion like equation with BFKL kernels as noted originally by Mueller [27, 28]. This evolution maps onto an evolution in an emergent AdS<sub>5</sub> space, spanned by the 1 + 1 longitudinal directions plus additional transverse directions.

These observations extend to strong 't Hooft coupling and large  $N_c$ , where the evolution of the partial trace of the reduced density matrix, is captured by the evolution of the tachyonic mode of a boosted string in AdS<sub>5</sub> space. The largest eigenvalues of the one-body reduced density matrix, gives a good account of the hadronic multiplicities currently reported in  $pp$  collisions at the largest  $\sqrt{s}$  at the LHC. The eigenvalues of the two-body reduced density matrix, may account for the multiplicities from  $pp$  processes with a double rapidity gap.

Finally, the boosted string is characterized by an Unruh-like temperature  $T = (y/b)/2\pi$  on the world-sheet (with  $b$  in arbitrary  $D_\perp$  dimensions) [15, 37]. The string effective thermal entropy, is the entanglement entropy induced by small- $x$  gluons in quarkonium-quarkonium scattering, extended to strong coupling. Feynman wee and perturbative partons at low- $x$  [6], are dual to Susskind-Thorn non-perturbative string bits [12–14], in a long



string undergoing large boosts. For the latter, the entanglement is captured geometrically by the hyperbolic string world-sheet [40].

### Acknowledgements

This work was supported by the U.S. Department of Energy under Contract No. DE-FG-88ER40388, and by the Priority Research Area SciMat under the program Excellence Initiative Research University at the Jagiellonian University in Krakow.

- 
- [1] M. Srednicki, Entropy and area, *Phys. Rev. Lett.* **71**, 666 (1993), [arXiv:hep-th/9303048](#).
  - [2] P. Calabrese and J. L. Cardy, Entanglement entropy and quantum field theory, *J. Stat. Mech.* **0406**, P06002 (2004), [arXiv:hep-th/0405152](#).
  - [3] H. Casini, C. D. Fosco, and M. Huerta, Entanglement and alpha entropies for a massive Dirac field in two dimensions, *J. Stat. Mech.* **0507**, P07007 (2005), [arXiv:cond-mat/0505563](#).
  - [4] M. B. Hastings, An area law for one-dimensional quantum systems, *J. Stat. Mech.* **0708**, P08024 (2007), [arXiv:0705.2024 \[quant-ph\]](#).
  - [5] P. Calabrese and J. Cardy, Entanglement entropy and conformal field theory, *J. Phys. A* **42**, 504005 (2009), [arXiv:0905.4013 \[cond-mat.stat-mech\]](#).
  - [6] R. P. Feynman, The behavior of hadron collisions at extreme energies, *Conf. Proc. C* **690905**, 237 (1969).
  - [7] E. A. Kuraev, L. N. Lipatov, and V. S. Fadin, The Pomeranchuk Singularity in Nonabelian Gauge Theories, *Sov. Phys. JETP* **45**, 199 (1977).
  - [8] I. I. Balitsky and L. N. Lipatov, The Pomeranchuk Singularity in Quantum Chromodynamics, *Sov. J. Nucl. Phys.* **28**, 822 (1978).
  - [9] L. N. Lipatov, Small x physics in perturbative QCD, *Phys. Rept.* **286**, 131 (1997), [arXiv:hep-ph/9610276](#).
  - [10] I. Balitsky, Operator expansion for high-energy scattering, *Nucl. Phys. B* **463**, 99 (1996), [arXiv:hep-ph/9509348](#).
  - [11] Y. V. Kovchegov, Small x F(2) structure function of a nucleus including multiple pomeron exchanges, *Phys. Rev. D* **60**, 034008 (1999), [arXiv:hep-ph/9901281](#).
  - [12] L. Susskind, String theory and the principles of black hole complementarity, *Phys. Rev. Lett.* **71**, 2367 (1993), [arXiv:hep-th/9307168](#).
  - [13] L. Susskind, Strings, black holes and Lorentz contraction, *Phys. Rev. D* **49**, 6606 (1994), [arXiv:hep-th/9308139](#).
  - [14] C. B. Thorn, Calculating the rest tension for a polymer of string bits, *Phys. Rev. D* **51**, 647 (1995), [arXiv:hep-th/9407169](#).

- [15] A. Stoffers and I. Zahed, Holographic Pomeron and Entropy, *Phys. Rev. D* **88**, 025038 (2013), [arXiv:1211.3077 \[nucl-th\]](#).
- [16] D. E. Kharzeev and E. M. Levin, Deep inelastic scattering as a probe of entanglement, *Phys. Rev. D* **95**, 114008 (2017), [arXiv:1702.03489 \[hep-ph\]](#).
- [17] N. Armesto, F. Dominguez, A. Kovner, M. Lublinsky, and V. Skokov, The Color Glass Condensate density matrix: Lindblad evolution, entanglement entropy and Wigner functional, *JHEP* **05**, 025, [arXiv:1901.08080 \[hep-ph\]](#).
- [18] G. Dvali and R. Venugopalan, Classicalization and unitarization of wee partons in QCD and Gravity: The CGC-Black Hole correspondence, (2021), [arXiv:2106.11989 \[hep-th\]](#).
- [19] Y. Qian and I. Zahed, Stretched String with Self-Interaction at High Resolution: Spatial Sizes and Saturation, *Phys. Rev. D* **91**, 125032 (2015), [arXiv:1411.3653 \[hep-ph\]](#).
- [20] Y. Qian and I. Zahed, Stretched string with self-interaction at the Hagedorn point: Spatial sizes and black holes, *Phys. Rev. D* **92**, 105001 (2015), [arXiv:1508.03760 \[hep-ph\]](#).
- [21] E. Shuryak and I. Zahed, Regimes of the Pomeron and its Intrinsic Entropy, *Annals Phys.* **396**, 1 (2018), [arXiv:1707.01885 \[hep-ph\]](#).
- [22] Y. Liu, M. A. Nowak, and I. Zahed, Entanglement entropy and flow in two dimensional QCD:parton and string duality, (2022), [arXiv:2202.02612 \[hep-ph\]](#).
- [23] K. Kutak, Gluon saturation and entropy production in proton–proton collisions, *Phys. Lett. B* **705**, 217 (2011), [arXiv:1103.3654 \[hep-ph\]](#).
- [24] H. Bremermann, in *Proceedings of the Fifth Berkeley Symposium on Mathematical Statistics and Probability*, Eds. Le Cam, Lucien Marie and Neyman, Jerzy, Vol. 3 (Univ of California Press, 1967).
- [25] J. D. Bekenstein, Energy Cost of Information Transfer, *Phys. Rev. Lett.* **46**, 623 (1981).
- [26] A. Dumitru and E. Kolbusz, Quark and gluon entanglement in the proton on the light cone at intermediate  $x$ , (2022), [arXiv:2202.01803 \[hep-ph\]](#).
- [27] A. H. Mueller, Soft gluons in the infinite momentum wave function and the BFKL pomeron, *Nucl. Phys. B* **415**, 373 (1994).
- [28] A. H. Mueller, Unitarity and the BFKL pomeron, *Nucl. Phys. B* **437**, 107 (1995), [arXiv:hep-ph/9408245](#).
- [29] X. Ji and Y. Liu, Computing Light-Front Wave Functions Without Light-Front Quantization: A Large-Momentum Effective Theory Approach, (2021), [arXiv:2106.05310 \[hep-ph\]](#).
- [30] Y. V. Kovchegov and E. Levin, *Quantum chromodynamics at high energy*, Vol. 33 (Cambridge University Press, 2012).
- [31] M. A. Nowak and P. Wegrzyn, eds., *Bosonization and conformal field theories in high-energy and condensed matter physics. Proceedings, 35th Cracow School of Theoretical Physics, Zakopane, Poland, June 4-14, 1995*, Vol. 26 (1995).
- [32] R. Kirschner, Small  $x$  physics, *Acta Phys. Polon. B* **26**, 1961 (1995).

- [33] M. Rho, S.-J. Sin, and I. Zahed, Elastic parton-parton scattering from AdS / CFT, *Phys. Lett. B* **466**, 199 (1999), [arXiv:hep-th/9907126](#).
- [34] R. A. Janik and R. B. Peschanski, Minimal surfaces and Reggeization in the AdS / CFT correspondence, *Nucl. Phys. B* **586**, 163 (2000), [arXiv:hep-th/0003059](#).
- [35] J. Polchinski and M. J. Strassler, Deep inelastic scattering and gauge / string duality, *JHEP* **05**, 012, [arXiv:hep-th/0209211](#).
- [36] R. C. Brower, J. Polchinski, M. J. Strassler, and C.-I. Tan, The Pomeron and gauge/string duality, *JHEP* **12**, 005, [arXiv:hep-th/0603115](#).
- [37] G. Basar, D. E. Kharzeev, H.-U. Yee, and I. Zahed, Holographic Pomeron and the Schwinger Mechanism, *Phys. Rev. D* **85**, 105005 (2012), [arXiv:1202.0831 \[hep-th\]](#).
- [38] R. A. Janik and P. Laskoś-Grabowski, Approaching the BFKL pomeron via integrable classical solutions, *JHEP* **01**, 074, [arXiv:1311.2302 \[hep-th\]](#).
- [39] A. Stoffers and I. Zahed, Holographic Pomeron: Saturation and DIS, *Phys. Rev. D* **87**, 075023 (2013), [arXiv:1205.3223 \[hep-ph\]](#).
- [40] Y. Liu and I. Zahed, Entanglement in Regge scattering using the AdS/CFT correspondence, *Phys. Rev. D* **100**, 046005 (2019), [arXiv:1803.09157 \[hep-ph\]](#).
- [41] V. Khachatryan *et al.* (CMS), Charged Particle Multiplicities in  $pp$  Interactions at  $\sqrt{s} = 0.9, 2.36, \text{ and } 7$  TeV, *JHEP* **01**, 079, [arXiv:1011.5531 \[hep-ex\]](#).
- [42] K. Zhang, K. Hao, D. Kharzeev, and V. Korepin, Entanglement entropy production in deep inelastic scattering, *Phys. Rev. D* **105**, 014002 (2022), [arXiv:2110.04881 \[quant-ph\]](#).
- [43] K. Kutak and P. Surówka, Nonlinear evolution of unintegrated gluon density at large values of coupling constant, *Phys. Rev. D* **89**, 026007 (2014), [arXiv:1309.3450 \[hep-ph\]](#).